

Machine Learning for SAT: Restricted Heuristics and New Graph Representations

Mikhail Shirokikh², Ilya Shenbin¹,
Anton Alekseev^{1,2}, and Sergey Nikolenko^{1,2}

¹Steklov Institute of Mathematics at St. Petersburg,
St. Petersburg, Russia

²St. Petersburg State University, St. Petersburg, Russia

July 19, 2023

Abstract

Boolean satisfiability (SAT) is a fundamental NP-complete problem with many applications, including automated planning and scheduling. To solve large instances, SAT solvers have to rely on heuristics, e.g., choosing a branching variable in DPLL and CDCL solvers. Such heuristics can be improved with machine learning (ML) models; they can reduce the number of steps but usually hinder the running time because useful models are relatively large and slow. We suggest the strategy of making a few initial steps with a trained ML model and then releasing control to classical heuristics; this simplifies cold start for SAT solving and can decrease both the number of steps and overall runtime, but requires a separate decision of when to release control to the solver. Moreover, we introduce a modification of *Graph-Q-SAT* tailored to SAT problems converted from other domains, e.g., open shop scheduling problems. We validate the feasibility of our approach with random and industrial SAT problems.

1 Introduction

Boolean satisfiability (SAT), i.e., deciding whether a Boolean formula in conjunctive normal form (CNF) is satisfiable, is the archetypal NP-complete problem, with numerous applications in computer science. There exist several different classes of approaches to solving SAT: stochastic local search (SLS), Davis–Putman–Logemann–Loveland solvers (DPLL), conflict-driven clause learning (CDCL), ordered binary decision diagrams (OBDD), and others [10]. All known methods are, naturally, exponential in the worst case, and to solve large problems in practice they need to use various heuristics that have a crucial impact

on performance: SLS solvers choose a variable to flip, DPLL and CDCL solvers choose branching variables and their assignments, OBDD-based solvers choose clauses for conjunction and variables for projections. In all cases, key decisions have to be made under uncertainty, which opens up possibilities for using machine learning (ML) techniques to improve SAT and SMT solvers.

Various ML-based techniques have arisen to make better heuristic decisions (see “Related work”). However, they introduce another tradeoff: ML models are usually computationally heavy, and benefits in terms of the number of solver iterations have to be weighted against extra costs the model incurs. Here, we consider *Graph-Q-SAT* [13], a model that can reduce the number of iterations for a CDCL solver but that is based on a reinforcement learning (RL) agent with a complex graph neural network (GNN) inside.

In this work, we propose a technique for finding this tradeoff: we suggest to make only a few initial steps with a trained RL agent and then release control to classical heuristics. We consider several modifications of this idea: constant number of “heavy” steps, a separate action in the RL agent trained to release control, and a separate head in the model to make this decision. We introduce a novel modification with an action pool that uses the (heavy) RL agent once to predict several actions that can be used for several steps. Moreover, we propose a new approach tailored specifically for SAT instances originating from other optimization problems such as open shop scheduling (OSSP). Namely, we construct a GNN whose graph corresponds not to the SAT formula but to the original OSSP instance; this greatly reduces the size of the graph and improves the results in SAT solving. We validate our approaches with an evaluation study on both random and industrial SAT instances.

The paper is organized as follows. Section 2 surveys related work on machine learning approaches to SAT. Section 3 introduces *Graph-Q-SAT* (Section 3.1) and our novel modifications for it (Section 3.2). Section 4 reports the experimental setup and datasets and specifies several novel implementation modifications that further improve *Graph-Q-SAT*. Section 5 presents and discusses the results of our evaluation study, and Section 6 concludes the paper.

2 Related work

SAT is a classification problem; end-to-end machine learning (ML) approaches have been proposed by Devlin and O’Sullivan [6] and with graph neural networks (GNN) by Selsam et al. [24], a method later extended to Circuit-SAT by Amizadeh et al. [1] and MAX-SAT by Liu et al. [17] and improved with recurrent neural networks by Ozolins et al. [21]. However, while a satisfying assignment can be verified, end-to-end solutions for an exact combinatorial problem via statistical methods cannot replace a complete solver, i.e., cannot make sure that a formula is unsatisfiable.

Instead of an end-to-end replacement, ML can be used to augment complete SAT solvers by enhancing their *heuristics*. SAT solvers—Davis-Putnam-Logeman-Loveland (DPLL), conflict-driven clause learning (CDCL), and stochas-

tic local search (SLS)—have decisions that have to be made during operation with incomplete information, usually recursively. Such decisions can be improved with ML. Boolean variables initialization has been improved by Wu et al. [33]; in SLS solvers, variable re-initialization is called upon every restart, so Zhang et al. [35] train a neural network to improve SLS initial assignments. Nejati et al. [20] learned restart strategies for CDCL solvers while Han et al. [8] predicted glue variables for the *CaDiCaL* solver previously proposed by Biere et al. [3].

The most important direction here is *variable selection* for branching in DPLL and CDCL solvers and flipping in SLS solvers. For DPLL and CDCL, the goal is to improve over the *Variable State Independent Decaying Sum* (VSIDS) heuristic originally introduced in the *Chaff* solver by Moskewicz et al. [19] that favors recently learned clauses based on specially introduced activity scores; Biere and Frölich [4] survey VSIDS variations. Selsam et al. [23] learn to predict the unsatisfiable core of a formula, using predictions to re-rank variables for branching; Jaszczur et al. [12] use a GNN in a similar way, while Han [9] prioritizes variables that often occur in DRAT proofs, learning to predict this fact.

However, the main downside of ML heuristics for solving SAT is the trade-off between reducing the number of steps and the time required to make predictions with the help of the heavyweight modern machine learning models. Therefore, while most works report significant reductions in the number of iterations from the use of ML-improved heuristics, one should also track the actual running time of the solver with and without these heuristics on equivalent hardware, and most ML methods have limited usability in practice due to computational inefficiency: a heavy neural network has to be used on every branching step. *NeuroComb* proposed by Wang et al. [31] uses GNNs only for preprocessing, running inference once per input formula (*static* predictions). Many works use reinforcement learning (RL) [27] to learn heuristics based on the running time or number of iterations as a reward. In particular, Yolcu and Póczos [34] use RL for SLS solvers to choose flip variables, Han [8] extends *NeuroCore* with RL, Liang et al. [15, 16] apply multi-armed bandits as branching heuristics, Lagoudakis and Littman [14] use TD-learning to select a branching heuristic given the current state, while Nejati et al. [20] apply multi-armed bandits to choose a restart strategy.

Graph-Q-SAT by Kurin et al. [13] utilizes Q-learning for branching heuristics in CDCL solvers via a Markov decision process (MDP) whose states are defined by unassigned variables and unsatisfied clauses with these variables; we will describe this approach in detail below. We also note here that Wang et al. [30] already introduced a similar MDP formulation, which did not use GNNs and instead was based on *AlphaGo Zero*. Interestingly, games such as Go and chess indeed give rise to computationally intractable problems, e.g., the game of Go on an $n \times n$ board has been shown to be EXPTIME-complete [22] and chess to be PSPACE-complete [26], so these two directions of research are not as different as it might seem.

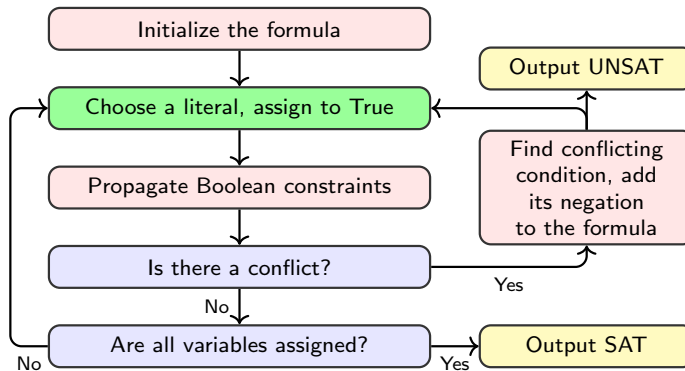


Figure 1: CDCL solver operation: choosing an assignment is a heuristic step that can be improved by machine learning.

3 Proposed method

3.1 Graph-Q-SAT

In this work, we build upon the *Graph-Q-SAT* approach by Kurin et al. [13] that uses Q-learning for branching heuristics in CDCL solvers [25]. A CDCL solver operates as shown in Fig. 1: on every step, it

- chooses a literal (variable and its value) to assign,
- then propagates Boolean constraints such as, e.g., unit clauses (clauses with one literal) that lead to more necessary assignments.

If the solver arrives at a conflict (empty clause), it finds the conflicting condition (a cut in the implication graph), backtracks to the assignment where it occurred, and adds the clause representing its negation to the formula. If the algorithm has backtracked from both possible assignments of a variable, the formula is unsatisfiable. If all variables have been assigned with no conflict, the solver has found a satisfying assignment.

On every iteration, a CDCL solver has to choose a literal. This part is a heuristic, and choosing correct variables can lead to exponential speedups in the running time and number of iterations needed for both SAT and UNSAT instances, so this is the place where ML-based heuristics may help.

Graph-Q-SAT is a reinforcement learning method that learns to choose literals by treating the problem as a Markov decision process (MDP):

- the task $\tau \sim D(\phi, (\text{un})\text{SAT}, n_{\text{vars}}, n_{\text{clauses}})$ is a SAT problem, sampled from a task family ϕ with known satisfiability status and given number of variables and clauses;
- each state of the MDP is defined by unassigned variables and unsatisfied clauses with these variables;

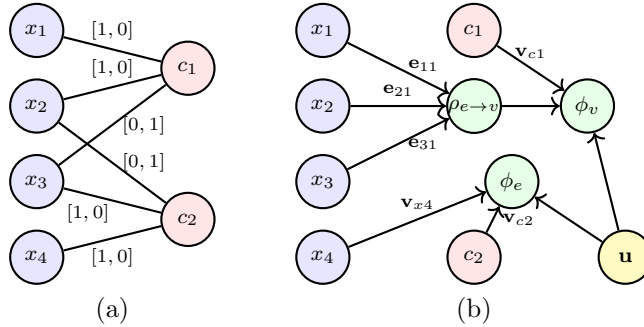


Figure 2: *Graph-Q-SAT*: (a) the variable-clause graph for the formula $(x_1 \vee x_2 \vee \neg x_3) \wedge (\neg x_2 \vee x_3 \vee x_4)$; (b) computation of sample GNN updates for \mathbf{v}_{c1} (top) and $\mathbf{e}_{x4,c2}$ (bottom).

- actions available to the agent are the choice of a variable and its polarity;
- a terminal state is reached when either a satisfying assignment or an unsat core is found, and the final reward is 1 with a discount factor $\gamma < 1$ to reward solving SAT faster.

This is a sufficiently general formulation that has been only slightly modified in other works that apply RL to SAT. *Graph-Q-SAT* uses *Q-learning* that learns to predict utilities for each action; for SAT, it means that for a given formula, *Graph-Q-SAT* learns to predict expected utilities $Q(l)$ (running time rewards) based on the formula structure for each literal l ; we can choose $\arg \max_l Q(l)$ as the next literal to assign during inference. See, e.g., Mnih et al. [18] for a detailed discussion of (deep) Q-learning.

To estimate $Q(l)$, *Graph-Q-SAT* uses a *graph neural network* (GNN) [2], which is a common theme in ML for SAT [24, 34]. It uses the variable-clause graph to represent formulas, i.e., a formula with n variables and m clauses corresponds to a bipartite graph $G = (V, E)$ with n and m variables in each part (see Fig. 2a). An edge $(x_i, c_j) \in E$ means that x_i occurs in the clause c_j ; an edge is labeled $[0, 1]$ if c_j contains the positive literal x_i and $[1, 0]$ if it contains $\neg x_i$.

On each step, GNN propagates information along the edges of G , updating the embeddings of edges \mathbf{e}_{ij} , embeddings of vertices \mathbf{v}_i , and a global context vector \mathbf{u} . The network is defined by update functions ϕ_e, ϕ_v, ϕ_u that change the embeddings and aggregation functions $\rho_{e \rightarrow v}, \rho_{e \rightarrow u}, \rho_{v \rightarrow u}$ that combine the embeddings of adjacent entities.

Formally, on every iteration the GNN updates (see Fig. 2b)

$$\begin{aligned}
 \mathbf{e}_{ij} &:= \phi_e(\mathbf{u}, \mathbf{e}_{ij}, \mathbf{v}_i, \mathbf{v}_j) \quad \forall e_{ij} \in E, \\
 \mathbf{v}_i &:= \phi_v(\mathbf{u}, \mathbf{v}_i, \rho_{e \rightarrow v}(\{\mathbf{e}_{ki} \mid e_{ki} \in E\})) \quad \forall v_i \in V, \\
 \mathbf{u} &:= \phi_u(\mathbf{u}, \rho_{e \rightarrow u}(\{\mathbf{e} \mid e \in E\}), \rho_{v \rightarrow u}(\{\mathbf{v} \mid v \in V\})),
 \end{aligned}$$

repeating until convergence or until it is stopped. Sample computations are illustrated in the graph shown in Fig. 2b.

The functions are parameterized with neural networks, trained with back-propagation on the learning phase. The original *Graph-Q-SAT* uses the *Encoder-Core-Decoder* architecture that consists of three significantly different parts. The encoder and decoder do not aggregate along the edges; they apply linear layers with *ReLU* activation functions to the feature vectors \mathbf{v} , \mathbf{e} , and \mathbf{u} . The core is located between them and consists of 4 GNN layers as described above. Interestingly, while the original *Graph-Q-SAT* code does have generic encoder and decoder parts implemented, the version introduced by Kurin et al. [13] has no hidden layers in the encoder and decoder.

As the underlying solver *Graph-Q-SAT* uses *MiniSAT* [7], an award-winning CDCL solver that chooses the next branching literal based on their *activity scores*, with a variation of the *Variable State Independent Decaying Sum* (VSIDS) heuristic; it favors recently learned clauses, increasing activity scores for variables in recent clauses and decaying them with time. *Graph-Q-SAT* replaces VSIDS scores with predicted values of $Q(l)$.

3.2 Our modifications

We have made several modifications and improvements for the *Graph-Q-SAT* framework. First and most importantly, we note that running a graph neural network on every step of SAT solving is a very resource-intensive task; even if it helps further reduce the number of steps a little, it certainly hurts the running time, usually drastically. The most influential decisions come at the beginning, and this is exactly when classical SAT solving heuristics such as MiniSAT activity scores are not yet meaningful (they don't yet have enough statistics). Therefore, we consider two ways of limiting the time:

- (1) running *Graph-Q-SAT* for a fixed number of steps and then releasing control to MiniSAT;
- (2) learning when to release control to MiniSAT, i.e., training a separate head that predicts this.

We also experimented with running the model once per several steps, but these experiments did not bring improvements and are not reported below.

Second, we propose one more way to reduce the number of calls to the agent, namely to utilize every run of the agent network in a more efficient way. The graph that represents the current formula changes only slightly after each step of the SAT solving agent. Therefore, we can assume that the list of actions with the highest Q-values in most cases will also change only slightly, which is confirmed by experiments. Following this motivation, we propose to keep top k actions that correspond to the highest Q-values and perform these actions sequentially (ignoring actions that have become invalid by the time of their execution). Such a policy is used at test time only, not at train time. The number k , i.e., the number of actions per agent run, is a constant hyperparameter, although we note

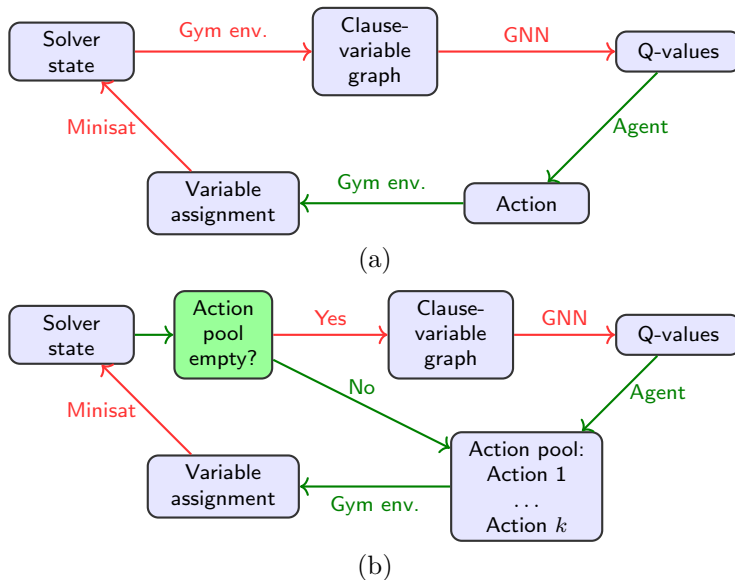


Figure 3: Using the action pool: (a) regular *Graph-Q-SAT* operation; (b) our modification with the action pool. Green arrows show “fast” operations; red arrows, “slow” operations that incur significant computational costs.

as a possible extension for future work that the number k could also be adaptive. The value of k should be large enough to get sufficient runtime acceleration in SAT solving while remaining small enough so that the environment does not change too much and the values of the Q function remain relevant. We call this set of precomputed actions the *action pool*; the resulting workflow is shown in Fig. 3b in comparison with the regular *Graph-Q-SAT* workflow (Fig. 3a).

Third, we have experimented with *Graph-Q-SAT* architectures. In the final version, we:

- turned on the encoder and decoder parts;
- increased the number of core layers from 4 to 13;
- increased the depth of core layers from 1 to 2;
- added a separate “release control” action predicted with two linear layers over the penultimate layer of the network.

Third, Kurin et al. [13] use a MiniSAT implementation that serves as the RL environment for *Graph-Q-SAT*, and this significantly increases the runtime. Since we release control to MiniSAT and do not return to RL, we are able to use the original MiniSAT after release, which has sped up SAT solving by a factor of about 10x; in all experiments, we report the runtimes of our version.

4 Experimental setup

4.1 Model setup and training

Similar to Kurin et al. [13], we used Random 3-SAT instances during training, with 50 variables and 218 clauses each (close to the phase transition threshold), and coloring problems for random graphs with 75 vertices and 180 edges; see also the SATLIB benchmark [11].

Since we need to learn to switch between RL and VSIDS heuristics, we have changed the rewards. With constant $-p$ reward for every step, as in the original Graph-Q-SAT [13], the agent would have no motivation to flip the switch as long as his variable assignments are better than random. Therefore, instead of a constant penalty $-p$ for every iteration we used $-t$, where t is the CPU time in milliseconds for this step (higher for RL and lower for VSIDS).

We also turned off discounting for Q values (set $\gamma = 1$) to motivate the agent to look ahead to long-term costs and switched to Double DQN instead of regular DQN; both of these changes significantly improved the agent’s behaviour in our experiments.

We have also expanded the action space with a new one that releases control to VSIDS. During training, we force the agent to make a small constant number of steps n since otherwise for an untrained agent this action would always be preferable; the value of n did not have a significant effect on the results. We also replaced DQN learning with Double DQN [29], which stabilized the training process.

Note that the reward received after the switch varies over time, which does not match the conventional definition of MDPs. However, we can treat this model as an MDP as follows: suppose that at time t we have a valid action with reward r_t that switches control to VSIDS, and at time $t + 1$ we have a different action that does the same but obtains reward r_{t+1} . In the implementation, it turns out that parameters of the action with reward r_{t+1} are initialized by parameters of the action with reward r_t .

Each model is run three times on every task, and the tables show averaged results.

4.2 Evaluation datasets

For evaluation, we have chosen several traditional SAT datasets and generated open shop scheduling problems (OSSP).

SR(n). For random generation, we use the **SR**(n) distribution introduced by Selsam et al. [24]. To generate a random clause on n variables, **SR**(n) samples a small integer k with mean a little over 4, namely as a sum of two random variables

$$1 + \mathbf{Bernoulli}(0.7) + \mathbf{Geo}(0.4)$$

(since there should not be many 2-literal clauses), then samples k variables uniformly at random without replacement, and negates each one with probability

0.5.

The clauses c_i are consecutively generated and added to the SAT instance until the problem becomes unsatisfiable at step m . Since we know that it is only c_m that “breaks” satisfiability, negating any literal in c_m leads to a satisfiable formula with clauses $\{c_1, \dots, c_{m-1}, c'_m\}$; both $c_1 \wedge \dots \wedge c_{m-1} \wedge c'_m$ and $c_1 \wedge \dots \wedge c_m$ are added to the set. This is a standard distribution for SAT evaluation [24,34].

Industrial. This is the *maris05* subset of industrial problems from the SAT 2005 Competition benchmark¹.

OSSP datasets. Open shop scheduling is a standard scheduling problem; the task is to distribute the workload across a finite number of resources (machines). The workload is represented as a list of jobs; a job is essentially a set of order-independent operations that each must be processed on a certain machine, i.e., we need to schedule n jobs on m machines, where each of the n jobs has its own sequence of operations that have to be done within m machines, with the goal to optimize an objective function under constraints that can define termination times, delay times, or total flow times, among others. For each job, only one operation can be run at a given moment of time (i.e., jobs cannot be run “in parallel”), and each machine can be occupied with only one operation at a time. The timespans p_* required for each operation to be completed are given. The open shop scheduling problem (OSSP) is to find the schedule with the shortest *makespan*, i.e., the time interval between the start of work and the end of the last completed job. For 3 or more machines and 3 or more jobs, OSSP is known to be NP-hard [32].

We have generated a problem set proposed by Taillard [28]²; upper and lower bounds for the makespans are provided. For default conversion to CNF, we have chosen the Crawford-Baker encoding [5].

Specifically, the Crawford-Baker encoding enumerates all operations (a batch of work for a single job that has to be processed on a certain machine) and introduces the following Boolean *variables*:

- $sa_{i,t}$: “op i starts at time t or later”,
- $eb_{i,t}$: “op i ends by time t ”,
- $pr_{i,j}$: “op i precedes j ”.

The *constraints* are formulated as follows:

- $\forall_t sa_{i,t}$ for all operations i (each operation begins);
- $\forall_t eb_{i,t}, t > 0$ for all operations i (each operation ends);

¹Available at <https://zenodo.org/record/6528885>

²The generator (Pascal code) is available, e.g., at <http://people.brunel.ac.uk/~mastjjb/jeb/orlib/files/openshop.txt>

- $pr_{i,j} \vee pr_{j,i}$ for all operations i, j from the same job that are run on the same machine (they cannot run at the same time);
- $sa_{i,t} \rightarrow sa_{i,t-1}$ (an implication $a \rightarrow b$ is the disjunct $\neg a \vee b$) for all operations and all times t : if i starts at or after t , it starts at or after $t - 1$ (sa coherence);
- $eb_{i,t} \rightarrow eb_{i,t+1}$ for all possible i and t (eb coherence);
- $sa_{i,t} \rightarrow \neg eb_{i,t+p_i-1}$ for all i and t , where p_i is the processing time (operation i that started at time t or later cannot end before $t + p_i$);
- $sa_{i,t} \wedge pr_{i,j} \rightarrow sa_{j,t+p_i}$ for all i, j , and times t (operation j cannot start until operation i ends if i precedes j).

4.3 Graph-Q-SAT implementation modifications

We have made several modifications and improvements to the original *Graph-Q-SAT* implementation. First, the Graph-Q-SAT paper [13] makes comparisons against not the original *Minisat* solver but against **MinisatAgent**, an RL environment agent acting as *Minisat*. The number of steps remains the same, but the running time required for obtaining the results via **MinisatAgent** is significantly increased compared to the original *Minisat* solver.

To make our approach more feasible for real-life scenarios, we have added a new action to the environment (trainable in the *CoPilot* setting); when this action is triggered, the environment runs the original *Minisat* without rebuilding the graph or any calls to *Python* code whatsoever, which reduces runtimes very significantly.

In the case of choosing several sequential actions at once, the original *Graph-Q-SAT* implementation of both agent and environment resulted in the most time-consuming stage of each of the agent-environment interaction to become graph construction. But when we apply several predefined actions one by one, graph construction for every action is no longer necessary, and actions can be simply pulled from the action pool; thus, we made the action pool a part of the environment to avoid unnecessary computations.

5 Evaluation results

5.1 Results on standard SAT benchmarks

Table 1 shows the main results of our experimental evaluation. In Table 1:

- GQSAT is the original *Graph-Q-SAT* that uses the RL agent for 1, 2, 3, or 5 steps;
- GQSAT-2 denotes our extended *Graph-Q-SAT* architecture; both versions use our reimplementations of *Graph-Q-SAT* as described in Section 4.3;

Table 1: Evaluation on standard SAT benchmarks.

	# of model steps	Q-Activity	SR(300)		SR(500)		Industrial	
			Time	Steps	Time	Steps	Time	Steps
MiniSAT			0.069	655.1	1.292	14317.4	0.386	1033.9
GQSAT	1		0.096	656.9	1.270	13770.4	0.550	1220.2
	2		0.121	671.0	1.377	14294.4	0.516	991.0
	3		0.145	680.4	1.371	13918.8	0.597	1030.8
	5		0.180	640.7	1.429	13856.2	0.745	1070.8
GQSAT-2	1		0.119	644.6	1.425	14804.4	0.512	981.4
	2		0.160	645.6	1.486	14642.7	0.628	882.9
	3		0.203	654.7	1.693	15791.8	0.798	1074.3
	5		0.278	661.3	1.511	13099.7	1.097	1318.8
CoPilot	1		0.121	644.6	1.422	14804.4	0.558	1177.3
	2		0.160	645.6	1.487	14642.7	0.639	986.9
	3		0.201	654.7	1.708	15791.8	0.794	1026.7
	5		0.235	654.7	1.750	15791.8	0.904	1210.0
CoPilot	1	✓	0.123	644.6	1.419	14804.4	0.521	1019.3
	2	✓	0.160	645.6	1.477	14642.7	0.630	926.9
	3	✓	0.204	654.7	1.704	15791.8	0.797	1102.3
	5	✓	0.231	638.8	1.516	13759.8	0.973	1217.2

Table 2: Evaluation results for the action pool modification.

	# of model runs	Action pool size	SR(300)		SR(500)		Industrial	
			Time	Steps	Time	Steps	Time	Steps
MiniSAT			0.071	759.7	0.941	11292.7	1.881	4825.8
GQSAT	1		0.088	694.1	0.944	10443.8	1.867	4828.0
	2		0.124	611.6	0.848	9719.1	1.931	4805.6
	3		0.149	588.5	0.853	9507.9	2.166	4810.9
GQSAT-multistep	1	20	0.091	611.8	0.724	8718.5	1.842	4813.9
	2	20	0.107	571.4	0.721	8398.3	1.898	4532.0
	3	20	0.131	601.7	0.735	8409.9	1.983	4496.9
GQSAT-multistep	1	30	0.089	587.4	0.715	8508.3	1.771	4668.8
	2	30	0.110	600.6	0.732	8577.3	1.976	4734.7
	3	30	0.130	604.8	0.763	8681.3	3.332	7177.7

Table 3: Evaluation results for the new OSSP representation.

	# steps	5×5 OSSP		6×6 OSSP		7×7 OSSP	
MiniSAT		0.886	167.4	4.483	402.7	14.444	1153.6
GQSAT	1	1.557	165.8	5.643	406.5	16.978	1152.1
	2	2.174	169.7	7.201	420.5	19.028	1149.0
	3	2.787	164.6	8.926	431.1	22.281	1144.2
CoPilot with the new graph representation	1	0.890	154.7	4.423	406.8	14.423	1151.5
	2	1.080	170.2	4.677	403.4	14.869	1157.0
	3	1.254	171.0	5.303	387.3	16.350	1138.9

- MiniSAT denotes the GQSAT implementation where the RL model is not used;
- CoPilot is the GQSAT-2 model with an additional action for releasing control to MiniSAT, still with a bounded number of steps.

In all cases, MiniSAT is run with restarts; we report average running times and numbers of iterations. The table shows that restricting the number of RL-based steps can improve the number of steps while saving time compared to running it for a longer time; CoPilot can improve the results further.

Another important idea here is that even if we release control to MiniSAT, we have already spent time on constructing the model and getting its predictions on first steps. We can reuse the estimated Q functions in MiniSAT’s activity scores, thus helping it with cold start. For each variable x_i , we use $-\frac{1}{\max(Q(x_i), Q(\neg x_i))}$ as the initial value of its activity score, and then they are modified according to usual MiniSAT rules. The column “Q-activity” shows this variation of the model, yielding significant improvements.

5.2 ML for SAT with an action pool

Table 2 presents the results for our *Graph-Q-SAT* modification proposed in Section 3.2, where the agent chooses several actions at once (Fig. 3b). We show several values of the action pool size (number of “precomputed” actions) and numbers of model runs (phrased in this way because now a model run corresponds to several steps); MiniSAT is run without restarts in this table. Figure 4 shows sample more detailed results for the SR(500) benchmark family in terms of both number of model runs (Fig. 4a) and running time (Fig. 4b) shown as a function of the action pool size.

Table 2 shows that the proposed approach with the action pool combines a significant reduction in the number of steps (much more so than in Table 1) with virtually no loss in evaluation runtime; we note here that the neural networks involved in our experiments were run in their default *PyTorch* implementations without any optimization tricks, and in an industrial environment ML-assisted runtimes might become significantly faster.

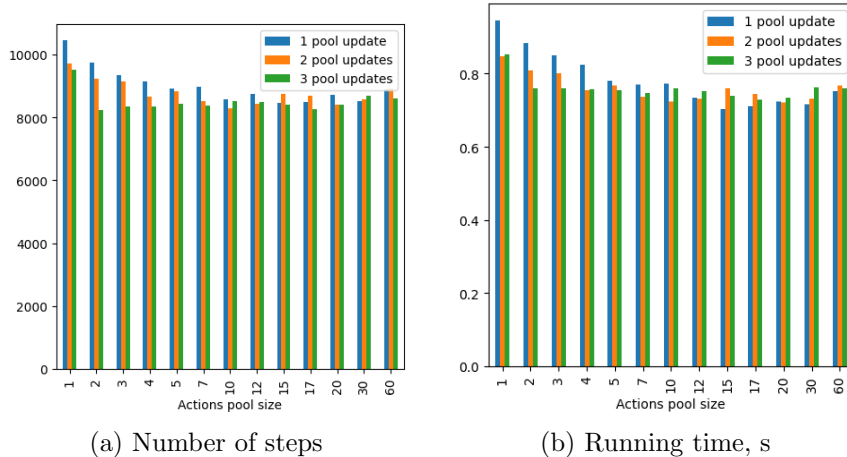


Figure 4: Experimental results for the SR(500) benchmark.

5.3 OSSP modification

The OSSP dataset highlights the main weakness of *Graph-Q-SAT*: even the smallest nontrivial (i.e., non-polynomial in the worst case) set, *ossp3-3*, has thousands of variables and clauses, which is not a problem for classical SAT solvers but bloats the *Graph-Q-SAT* model size and makes each RL agent step extremely expensive even during inference, let alone training the agent.

Hence, we propose a novel approach to solving OSSP via SAT with GNN-based heuristics. We still encode OSSP as SAT instances and use MiniSAT with neural heuristics, but we introduce a more compact graph representation for OSSP.

In our representation, the vertices correspond to operations, and every vertex is labeled with operation time, first possible timestamp when it can begin, and last timestamp when it has to finish (deadline). The first number is constant while the second and third depend on the current solver state; the labels are initialized with $(p_i, 1, T)$ and then are computed from the solver state on every step. We add an edge from vertex i to j if operation i can be done before j and i and j must be done on the same machine or belong to the same job (add edges between vertices whose operations cannot be done at the same time). A variable assignment now corresponds to choosing an edge: an edge from i to j means that operation i must be performed before op j , i.e., we set $pr_{ij} = \text{True}$.

The resulting graph is much smaller than the SAT graph for the Crawford-Baker encoding: for j jobs and m machines it has jm vertices and $O(jm(j+m))$ edges (note that this size does not depend on T) while the SAT formula has $O(j^2m^2 + jmT)$ variables and $O(j^2m^2(j+m) + T(jm)^2)$ clauses. For instance, a sample 7×7 OSSP task is encoded here with 49 vertices and 84 edges, while the SAT formula graph contains over 54K variables and 1.1M clauses. In fact, *Graph-Q-SAT* graphs for realistic sized problems become so large that they do

not fit into GPU memory for available hardware.

Table 3 shows that with the new graph representation, CoPilot operates almost as quickly as the original MiniSAT while reducing the number of iterations and much faster than *Graph-Q-SAT*; note that the difference is significant even though there were only at most 3 steps made with the model.

6 Conclusion

In this work, we have proposed an approach that limits heavy RL-based heuristics and finds the best tradeoffs between the number of iterations and their runtimes for SAT solvers. We have also introduced a novel graph representation for OSSP-based problems that greatly reduces model size and speeds up computations. In further work, we plan to extend this exciting direction, developing similar modifications for other optimization problems that can be reduced to Boolean satisfiability.

Acknowledgements

This research has been supported by the Huawei project TC20211214628.

References

- [1] S. Amizadeh, S. Matussevych, and M. Weimer. Learning to solve Circuit-SAT: An unsupervised differentiable approach. In *International Conference on Learning Representations*, 2018.
- [2] P. W. Battaglia, J. B. Hamrick, V. Bapst, A. Sanchez-Gonzalez, V. F. Zambaldi, M. Malinowski, A. Tacchetti, D. Raposo, A. Santoro, R. Faulkner, Ç. Gülçehre, H. F. Song, A. J. Ballard, J. Gilmer, G. E. Dahl, A. Vaswani, K. R. Allen, C. Nash, V. Langston, C. Dyer, N. Heess, D. Wierstra, P. Kohli, M. M. Botvinick, O. Vinyals, Y. Li, and R. Pascanu. Relational inductive biases, deep learning, and graph networks. *CoRR*, abs/1806.01261, 2018.
- [3] A. Biere, K. Fazekas, M. Fleury, and M. Heisinger. CaDiCaL, Kissat, Paracooba, Plingeling and Treengeling entering the SAT Competition 2020. In T. Balyo, N. Froleyks, M. Heule, M. Iser, M. Jarvisalo, and M. Suda, editors, *Proc. of SAT Competition 2020*, volume B-2020-1 of *Department of Computer Science Report Series B*, pages 51–53, 2020.
- [4] A. Biere and A. Fröhlich. Evaluating CDCL variable scoring schemes. In M. Heule and S. Weaver, editors, *Theory and Applications of Satisfiability Testing – SAT 2015*, pages 405–422, Cham, 2015. Springer International Publishing.

- [5] J. M. Crawford and A. B. Baker. Experimental results on the application of satisfiability algorithms to scheduling problems. In *Proceedings of the Twelfth AAAI National Conference on Artificial Intelligence*, pages 1092–1097, 1994.
- [6] D. Devlin and B. O’Sullivan. Satisfiability as a classification problem. In *Proc. of the 19th Irish Conf. on Artificial Intelligence and Cognitive Science*, 2008.
- [7] N. Eén and N. Sörensson. An extensible SAT-solver. In E. Giunchiglia and A. Tacchella, editors, *Theory and Applications of Satisfiability Testing*, pages 502–518, Berlin, Heidelberg, 2004. Springer Berlin Heidelberg.
- [8] J. M. Han. Enhancing SAT solvers with glue variable predictions. *arXiv:2007.02559*, 2020.
- [9] J. M. Han. Learning cubing heuristics for SAT from DRAT proofs. In *Conference on Artificial Intelligence and Theorem Proving (AITP)*, 2020.
- [10] S. B. Holden. Machine learning for automated theorem proving: Learning to solve sat and qsat. *Found. Trends Mach. Learn.*, 14(6):807–989, nov 2021.
- [11] H. Hoos and T. Stützle. *SATLIB: An online resource for research on SAT*, pages 283–292. 04 2000.
- [12] S. Jaszczur, M. Luszczuk, and H. Michalewski. Neural heuristics for SAT solving. *CoRR*, abs/2005.13406, 2020.
- [13] V. Kurin, S. Godil, S. Whiteson, and B. Catanzaro. Can Q-learning with graph networks learn a generalizable branching heuristic for a SAT solver? *Advances in Neural Information Processing Systems*, 33:9608–9621, 2020.
- [14] M. G. Lagoudakis and M. L. Littman. Learning to select branching rules in the DPLL procedure for satisfiability. *Electronic Notes in Discrete Mathematics*, 9:344–359, 2001.
- [15] J. Liang, V. Ganesh, P. Poupart, and K. Czarnecki. Exponential recency weighted average branching heuristic for SAT solvers. In *Proceedings of the AAAI Conference on Artificial Intelligence*, volume 30(1), 2016.
- [16] J. H. Liang, V. Ganesh, P. Poupart, and K. Czarnecki. Learning rate based branching heuristic for SAT solvers. In *International Conference on Theory and Applications of Satisfiability Testing*, pages 123–140. Springer, 2016.
- [17] M. Liu, F. Jia, P. Huang, F. Zhang, Y. Sun, S. Cai, F. Ma, and J. Zhang. Can graph neural networks learn to solve MaxSAT problem? *CoRR*, abs/2111.07568, 2021.

- [18] V. Mnih, K. Kavukcuoglu, D. Silver, A. Graves, I. Antonoglou, D. Wierstra, and M. A. Riedmiller. Playing Atari with deep reinforcement learning. *CoRR*, abs/1312.5602, 2013.
- [19] M. W. Moskewicz, C. F. Madigan, Y. Zhao, L. Zhang, and S. Malik. Chaff: Engineering an efficient SAT solver. In *Proceedings of the 38th annual Design Automation Conference*, pages 530–535, 2001.
- [20] S. Nejati, J. H. Liang, C. Gebotys, K. Czarnecki, and V. Ganesh. Adaptive restart and CEGAR-based solver for inverting cryptographic hash functions. In *Working Conference on Verified Software: Theories, Tools, and Experiments*, pages 120–131. Springer, 2017.
- [21] E. Ozolins, K. Freivalds, A. Draguns, E. Gaile, R. Zakovskis, and S. Kozlovics. Goal-aware neural SAT solver. In *2022 International Joint Conference on Neural Networks (IJCNN)*. IEEE, 2022.
- [22] J. M. Robson. The complexity of Go. In R. E. A. Mason, editor, *Information Processing 83, Proceedings of the IFIP 9th World Computer Congress, Paris, France, September 19-23, 1983*, pages 413–417. North-Holland/IFIP, 1983.
- [23] D. Selsam and N. Bjørner. Guiding high-performance SAT solvers with unsat-core predictions. In *International Conference on Theory and Applications of Satisfiability Testing*, pages 336–353. Springer, 2019.
- [24] D. Selsam, M. Lamm, B. Bünz, P. Liang, L. de Moura, and D. L. Dill. Learning a SAT solver from single-bit supervision. In *7th International Conference on Learning Representations, ICLR 2019*, 2019.
- [25] J. P. M. Silva, I. Lynce, and S. Malik. Conflict-driven clause learning SAT solvers. In A. Biere, M. Heule, H. van Maaren, and T. Walsh, editors, *Handbook of Satisfiability*, volume 185 of *Frontiers in Artificial Intelligence and Applications*, pages 131–153. IOS Press, 2009.
- [26] J. A. Storer. On the complexity of chess. *Journal of Computer and System Sciences*, 27(1):77–100, 1983.
- [27] R. S. Sutton and A. G. Barto. *Reinforcement learning: An introduction*. MIT press, 2018.
- [28] E. Taillard. Benchmarks for basic scheduling problems. *European Journal of Operational Research*, 64(2):278–285, 1993.
- [29] H. van Hasselt, A. Guez, and D. Silver. Deep reinforcement learning with Double Q-learning. *CoRR*, abs/1509.06461, 2015.
- [30] F. Wang and T. Rompf. From gameplay to symbolic reasoning: Learning SAT solver heuristics in the style of Alpha(Go) Zero. *arXiv:1802.05340*, 2018.

- [31] W. Wang, Y. Hu, M. Tiwari, S. Khurshid, K. L. McMillan, and R. Miikkulainen. NeuroComb: Improving SAT solving with graph neural networks. *CoRR*, abs/2110.14053, 2021.
- [32] D. P. Williamson, L. A. Hall, J. A. Hoogeveen, C. A. J. Hurkens, J. K. Lenstra, S. V. Sevast'janov, and D. B. Shmoys. Short shop schedules. *Operations Research*, 45(2):288–294, 1997.
- [33] H. Wu. Improving SAT-solving with machine learning. In *Proceedings of the 2017 ACM SIGCSE Technical Symposium on Computer Science Education*, pages 787–788, 2017.
- [34] E. Yolcu and B. Póczos. Learning local search heuristics for Boolean satisfiability. *Advances in Neural Information Processing Systems*, 32, 2019.
- [35] W. Zhang, Z. Sun, Q. Zhu, G. Li, S. Cai, Y. Xiong, and L. Zhang. NLocalSAT: Boosting local search with solution prediction. In *Proceedings of the Twenty-Ninth International Joint Conference on Artificial Intelligence*. International Joint Conferences on Artificial Intelligence Organization, jul 2020.